Talanta 190 (2018) 119–125

Contents lists available at ScienceDirect

Talanta

journal homepage: www.elsevier.com/locate/talanta

A chemiresistor sensor based on a cobalt(salen) metallopolymer for dissolved molecular oxygen

Camila F. Pereira, André Olean-Oliveira, Diego N. David-Parra, Marcos F.S. Teixeira*

Department of Chemistry and Biochemistry, School of Science and Technology - Sao Paulo State University (UNESP), Rua Roberto Simonsen 305, CEP 19060-900, Presidente Prudente, SP, Brazil

ARTICLE INFO

Keywords:
Metallopolymer
Chemical sensor
Impedance
Electrochemical device
Resistive sensor

ABSTRACT

A resistance detection device for dissolved molecular oxygen in aqueous solutions is prepared using a chemiresistor material as sensor platform. The chemiresistive circuit element is fashioned from a thin film of a cobalt-salen metallopolymer electrodeposited on a platinum electrode. Electrochemical impedance spectroscopy shows that the resistive and capacitive properties of the sensor platform depend on the presence of dissolved oxygen. The electrical circuit models are R(Q/R)(Q/R) and R(Q/R)(Q/RW) in the absence and presence of oxygen, respectively. The chemiresistor sensor exhibits good sensitivity (0.483 $k\Omega\,L\,mg^{-1}$), excellent reversibility and excellent linearity over a range of dissolved oxygen concentrations typically found under environmental conditions (2.72–40.9 $mg\,L^{-1}$). The sensor fabricated in this work can potentially serve as an alternative sensor for the detection of dissolved oxygen in environmental samples.

1. Introduction

The measurement of molecular oxygen is an essential part of monitoring mitochondrial activity in the biomedical field, microorganism cultivations in biotechnology industries and environmental water quality indices [1–3]. To address this challenge, the development of a low-cost, portable, easy-to-use chemical sensor with high detection sensitivity and real-time operability is being widely pursued. However, the vast majority of chemical sensors reported in the literature are limited to electrochemical [4–8] and optical sensing platforms [9–12]. Furthermore, most of the chemiresistor sensors described in the literature are limited to atmospheric oxygen sensing [13–16]; but none sensor for dissolved oxygen detection in aqueous electrolyte solutions have been reported.

Herein, a catalytically active poly[Co(salen)] was used to develop a chemiresistor sensor for dissolved oxygen detection that can be employed in natural waters. The electropolymerization of metal(salen) complexes results in the formation of π-conjugated metallopolymers with interesting morphological properties [17–20]. These poly[metal(salen)] materials exhibit good electrical conductivity, thermal and mechanical stability, and catalytic activities for several organic and inorganic molecules. When a metallopolymer thin film is coated on the surface of a conductive substrate, the coordination complexes tend to be organized in molecular nanocolumns [17]. The metallopolymer columns can be used as a sensing platform for the dioxygen reaction based on their electrical conductivity properties. The selectivity of the sensor is greatly improved by the presence of cobalt in the nanostructured material; cobalt(II) complexes with Schiff bases can easily bind molecular dioxygen [21–24]. Electrochemical impedance spectroscopy (EIS) was performed to measure the impedance of metallopolymer films on a platinum electrode. Remarkably, due to the strong redox interactions between the metallopolymer and the molecular oxygen in solution, the film conductivity of the chemiresistor sensor varies as a function of the dissolved oxygen.

2. Experimental section

2.1. Manufacturing of the chemiresistor sensor

All the reagents had a high purity of ≥ 98% (Sigma Aldrich), and all the electrochemical measurements were performed using a μ-Autolab type III potentiostat/galvanostat (Eco Chemie).

The protocol used to fabricate the chemiresistor sensor was similar to a previously reported procedure with some slight changes [25]; the self-assembly solution consisted of 1.0 $mmol\,L^{-1}$ Co(II) 2,2′-{1,2-ethanediylbis[nitrilo(*E*)methylylidene]}diphenolate (Co(salen)) and 0.10 $mol\,L^{-1}$ tetrabutylammonium perchlorate in acetonitrile. The platinum electrode surface (0.071 cm^2) was polished to a mirror finish

* Corresponding author.
E-mail address: marcos.fs.teixeira@unesp.br (M.F.S. Teixeira).

https://doi.org/10.1016/j.talanta.2018.07.080
Received 30 May 2018; Received in revised form 22 July 2018; Accepted 24 July 2018
Available online 25 July 2018
0039-9140/

using an aqueous slurry of 0.05 μm alumina particles and then washed with water and isopropyl alcohol in an ultrasonic cleaner. Then, the electrode was subjected to cyclic potential scans between − 0.1 to + 1.4 V vs. SCE in 0.5 mol L^{-1} H_2SO_4 until stable cyclic voltammograms were obtained. Next, the chemiresistor material (poly[Co(salen)]) was prepared on the Pt electrode by electropolymerization in the self-assembly solution. Four cyclic voltammograms (Fig. S1) were obtained in the potential range of −0.5 to + 1.5 V vs. SCE (scan rate 0.1 V s^{-1}) under an N_2 atmosphere. The sensor platform was then washed with methanol to remove the excess complexes. The preparation procedure is shown in Fig. S2.

2.2. Resistance measurements and dissolved O_2 detection

The resistance of the sensor platform in a 0.5 mol L^{-1} KCl solution containing molecular oxygen was measured by EIS at an applied potential of −0.20 V vs. SCE at 25 °C. The EIS measurements were performed by applying an incident sine wave of 10 mV in the frequency range of 50 kHz to 0.1 Hz at 10 step dec^{-1} using a PalmSens 3 instrument interfaced to the PSTrace 5.2 software for control and data collection. The complex plane impedance spectra were analyzed using the ZPlot 2.4 software.

The resistive response curve of the sensor platform as a function of the dissolved oxygen concentration was obtained by absolute impedance measurements at 0.5 Hz. The dissolved oxygen was determined after adding an aliquot of Na_2SO_3 standard solution. The gas concentration was calculated based on the oxygen consumption by sulfite. The oxygen dissolved in environmental water samples was measured by direct absolute impedance measurements. The results were compared to those obtained with a commercial O_2 sensor.

3. Results and discussion

3.1. Characterization of the electrochemical behavior of the metallopolymer sensor

Cyclic voltammetry of the metallopolymer on the electrode surface (Fig. 1) was conducted at 25 °C under a nitrogen gas flow using a KCl solution as the supporting electrolyte. The Co(II)/Co(III) redox couple (E_{ap} = +0.14 V and E_{cp} = +0.05 V vs. SCE) of the poly[Co(salen)], especially the peak for the oxidation of Co(II) to Co(III), is not clearly observed. This result is very similar to those reported for cobalt metallopolymers in the literature [25–27]. Relatively weak

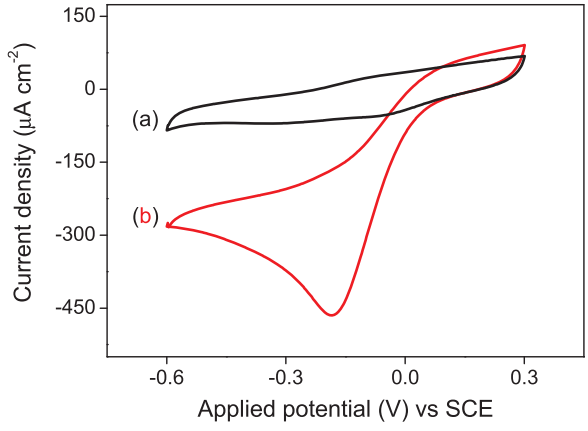

Fig. 1. Cyclic voltammetric response obtained for the platinum electrode coated with the metallopolymer in a 0.5 mol L^{-1} KCl solution: (**a**) in the absence of oxygen (**black line**); (**b**) under oxygen saturation conditions (**red line**). Scan rate = 5 mV s^{-1}. t = 25 °C. (For interpretation of the references to color in this figure legend, the reader is referred to the web version of this article.).

electrochemical response of the redox pair is related to the H_2O axial ligand effect on the Co(III) oxidation state [24,28]. The complex with the weak H_2O axial ligand tends to undergo slow interconversion between the Co(II) and Co(III) oxidation states. Oxidation and reduction peak currents are nearly unchanged in subsequent cycles of the potential. Concentration of the electroactive cobalt centers per area of the electrode was determined to be 1.2×10^{-11} mol cm^{-2} from the area under the cyclic voltammogram recorded at a scan rate of 5 mV s^{-1}. Under these electrochemical conditions and assuming that the molar volume is 237.2 (± 7.0) cm^3 mol^{-1} (ACD/Labs Percepta Platform), the film thickness of the resulting membrane is calculated to be approximately 2.8 ± 0.1 nm.

Fig. 1 also shows the catalytic activity of the metallopolymer for chemical dioxygen reduction. The results (curve b) were obtained in the presence of 40.1 mg L^{-1} of dissolved oxygen (saturated solution) in a 0.5 mol L^{-1} KCl solution in the potential range from + 0.3 to −0.6 V vs. SCE at a scan rate of 5 mV s^{-1}. The cyclic voltammogram reveals an increase in the cathodic current at −0.18 V vs. SCE, which can be assigned to the reduction of molecular oxygen in the aqueous solution. On the sensor surface, poly[Co(II)(salen)] forms an adduct with dioxygen (axial ligand), and the Co(II) center in the metallopolymer is subsequently oxidized to Co(III) (Eq. (1)). The adduct decomposes to produce Co(III) and hydrogen peroxide (Eq. (2)). The poly[Co(II)(salen)] form is then regenerated by the electroreduction of Co(III) (Eq. (3)), thus closing the catalytic cycle [29].

$$2Co^{(II)} + O_2 \rightleftharpoons 2Co^{(III)} - O_2^{2-} \quad (1)$$

$$2Co^{(III)} - O_2^{2-} + 2H^+ \rightleftharpoons Co^{(III)} + H_2O_2 \quad (2)$$

$$Co^{(III)} + e^- \rightleftharpoons Co^{(II)} \quad (3)$$

The electrocatalysis mechanism is not the main focus of this manuscript, and the conductivity of the polymer is discussed in the next section. However, molecular oxygen electroreduction on an uncoated platinum surface was studied by cyclic voltammetry under the same conditions (Fig. S3). The electrochemical response of the Pt surface is observed at −0.4 V vs. SCE. The overpotential of oxygen electroreduction increases significantly (by approximately 0.22 V) relative to that for the metallopolymer sensor. This result indicates that the presence of the metallopolymer on the electrode surface significantly enhances the efficiency of the molecular oxygen electroreduction process.

3.2. Impedance behavior of the metallopolymer sensor

The electrical properties of the metallopolymer film were investigated by electrochemical impedance spectroscopy (EIS) in an aqueous solution. The impedance spectra give important information about the resistive properties of the poly[Co(salen)] on platinum in the absence and presence of O_2. The electrolytic solution containing no dissolved oxygen was obtained by bubbling with N_2. Fig. 2A_1 shows the spectra of the metallopolymer/Pt system in a 0.5 mol L^{-1} KCl solution at −0.20 V vs. SCE. The complex plane impedance plot has two typical regions; the first region consists of a small semicircle at high frequencies (highlighted in Fig. 2A_2), and the second region consists of a larger semicircle that spans the middle- and low-frequency range. When the electrolytic solution does not contain oxygen, the impedance response can be modeled by an equivalent circuit (Fig. 2B_1) with five components, namely, the resistance of the electrolyte solution (R_Ω), $R_{ct\text{-}outer}/CPE_{dl}$ and $(R_{ct\text{-}inner})/CPE_{film}$, connected in series. $R_{ct\text{-}outer}$ is the resistance caused by the electron transfer process of the metallopolymer at the solution/polymer interface (outer interface), CPE_{dl} is the double layer capacitance, $R_{ct\text{-}inner}$ denotes the charge transfer resistance at the polymer/electrode interface (inner interface), and CPE_{film} is the film capacitance. CPE_{dl} and CPE_{film} are constant phase elements that account for the inhomogeneities in and roughness of the metallopolymer on the electrode surface.

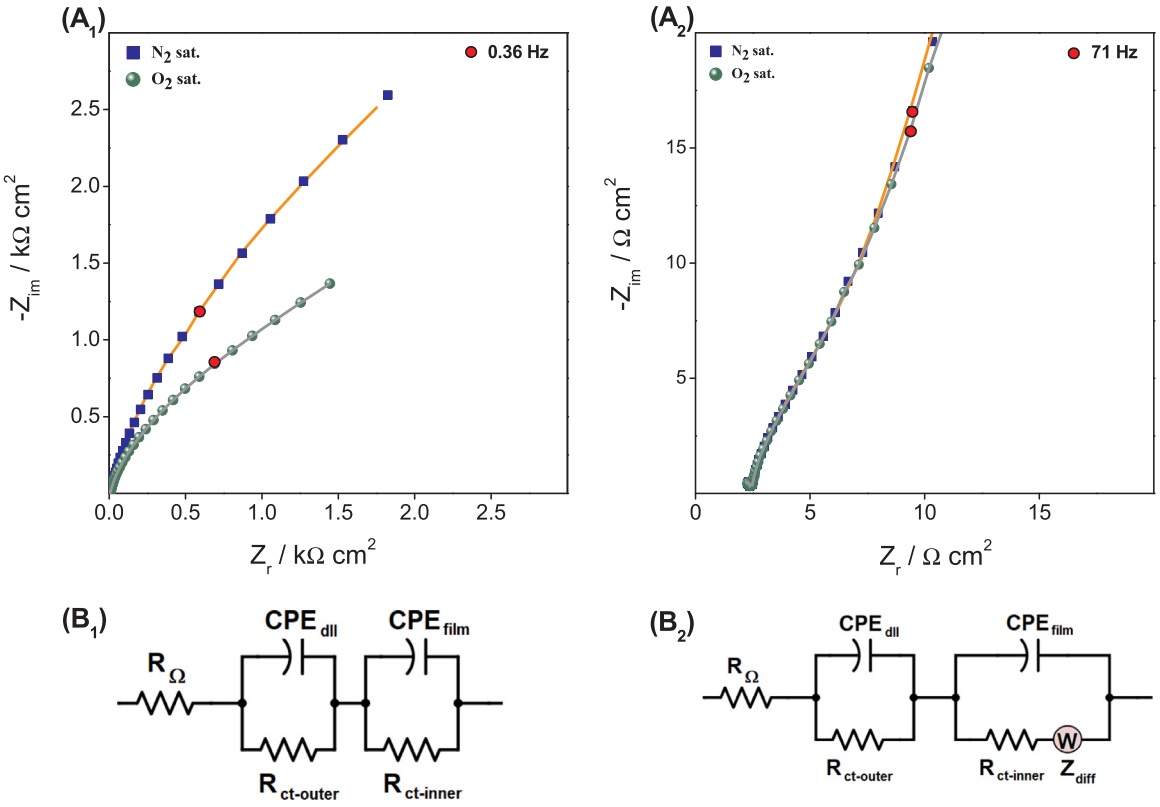

Fig. 2. ($\mathbf{A_1}$) and ($\mathbf{A_2}$) Nyquist impedance diagrams for the metallopolymer sensor in a 0.5 mol L^{-1} KCl solution saturated with N_2 (■) and O_2 (●) at an applied potential of −0.20 V vs. SCE (25 °C). The equivalent electrical circuits used to fit the complex plane impedance spectra in the absence and presence of oxygen are presented in ($\mathbf{B_1}$) and ($\mathbf{B_2}$), respectively. [O_2] = 41.1 mg L^{-1}.

Table 1
Parameters obtained by fitting the electrochemical impedance spectra of the chemiresistor material in the absence and presence of dissolved oxygen (41.1 mg L^{-1}) to the equivalent circuits in Fig. 2B_1 and 2B_2, respectively. t = 25 °C. The errors of the fits are less than 5%. R_Ω = 33.8 Ω.

	$R_{ct\text{-}outer}$ (Ω cm^2)	$R_{ct\text{-}inner}$	CPE_{dl} (μF cm^{-2} $s^{\alpha-1}$)	CPE_{film}	Z_{diff} (kΩ $s^{-\beta}$ cm^2)
N_2 sat. (B_1)	3.60	5364	0.373 (α = 0.9)	0.344 (α = 0.5)	–
O_2 sat. (B_2)	2.88	1902	0.339 (α = 0.9)	0.396 (α = 0.6)	0.809

The impedance spectrum obtained in the presence of oxygen was fitted by the equivalent circuit presented in Fig. 2B_2. It should be noted that for the impedance measurements at low frequencies, a Warburg diffusion element (Z_{diff}) was introduced. The Warburg impedance is due to the charge diffusion process, that is, it is related to the diffusion of the intercalated ions in the metallopolymer. Furthermore, molecular oxygen reaches the electrode surface through micropores in the coating, and an electrochemical reaction might occur at the inner surface of the porous layer (polymer/platinum interface). This diffusion behavior is not an ideal Warburg element because the dispersive number is less from 0.5 [30,31]. The non-ideal behavior can be attributed to the non-uniform penetration of molecular oxygen and the electrolyte, consequently an ionic displacement in porous polymer. The good fits of the impedance spectra to the electrical circuit models indicate the overall validity of applying these models to the sensor. The $R_{ct\text{-}inner}$ component decreases noticeably in the presence of dissolved oxygen (see Table 1).

By Bode plot (see Fig. 3) is possible to verify that there is no significant change in the shape of the spectrum for the poly[Co(salen)] on

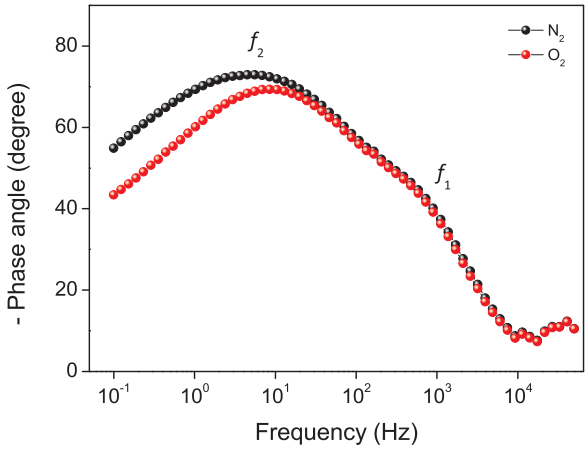

Fig. 3. The phase angle (Bode diagram) of the metallopolymer sensor in 0.5 mol L^{-1} KCl solution under nitrogen (**black circle**) and oxygen (**red cycle**) saturation conditions at an applied potential of −0.2 V vs. SCE. t = 25 °C. (For interpretation of the references to color in this figure legend, the reader is referred to the web version of this article.).

platinum in solution saturated with N_2 and O_2. The phase angle maximum at 450 Hz (f_1) attributed to the solution/metallopolymer interface was practically constant in the presence of molecular oxygen. Also, Bode plot reveals phase angle of 73° (f_2) for the metallopolymer/platinum interface at frequencies of < 10 kHz indicating that the material is primarily functioning as a capacitor in absence of dissolved oxygen. In this frequency range is associated with the charge accumulation inside the film pores, generating a region of charge difference between the counter-ions and the polarized electrode. The presence of dissolved oxygen resulted in a decrease of the phase angle and a small shift to

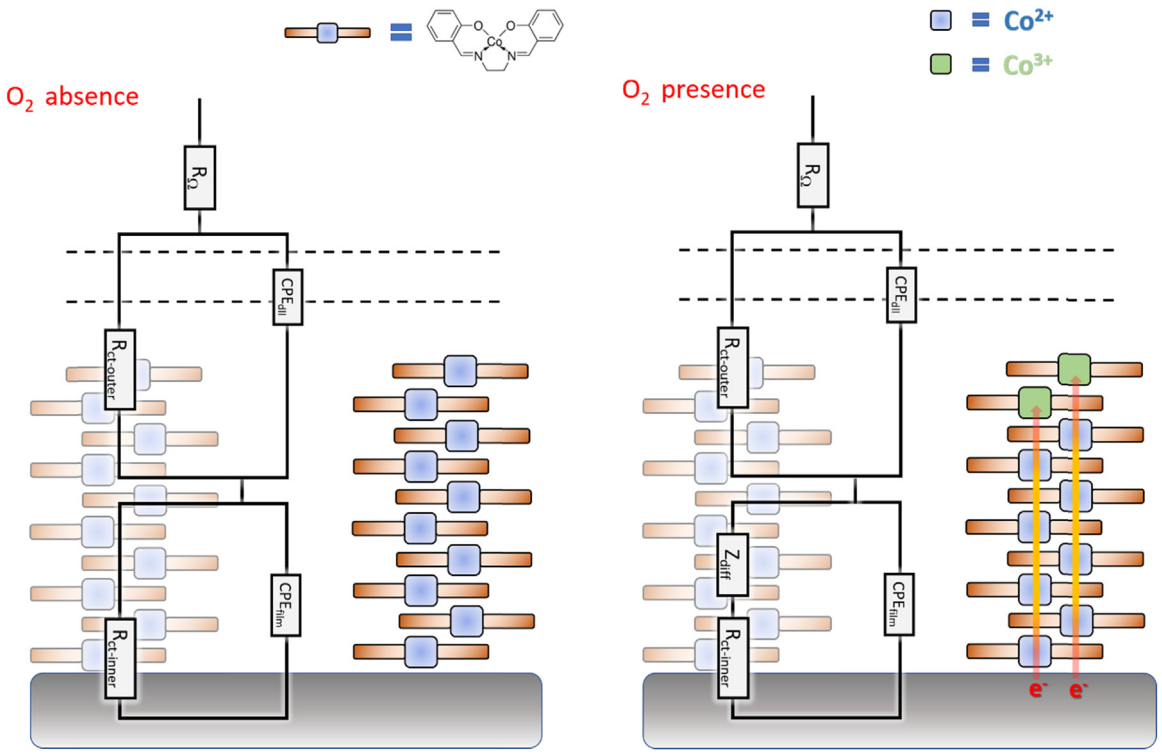

Scheme 1. Schematic representations of the equivalent circuit models used to fit the impedance data for the metallopolymer/platinum system in the absence and presence of dissolved oxygen. In the presence of O_2 (figure on the right), electron transfer occurs via hopping between the Co(II) and Co(III) valence states.

medium frequency of the phase angle maximum. This change is associated with the charge transfer of cobalt moieties with molecular oxygen.

The poly[Co(salen)] material consists of an extended three-dimensional network formed by axial coordination of d orbitals with the π orbitals of phenolate moiety of the adjacent complex. Furthermore, the conductivity occurs via π–d stacking interactions (inner-sphere ET through sequential hopping) [32–34]. The change in the oxidation state from Co(II) to Co(III) is crucial for increasing the conductivity of the metallopolymer (Scheme 1). The coordination of molecular oxygen in the axial position (dz^2 orbital) of the cobalt complex leads to the oxidation of Co(II) to Co(III). The mixed valency of the cobalt results in electronic coupling between sites with different formal charges, which leads to the rapid oscillation of charge throughout the polymer chain. Moreover, the system exhibits unique electronic properties due to the π–d stacking interactions (cobalt/aromatic rings). Zotti and coworkers [35] showed that electronic communication by band transport through a conjugated linkage is more effective than pure electron hopping.

The effects of the pH on the impedance response of the metallopolymer sensor were studied because the reduction of oxygen involves protons (see Eq. (2)). The plot of the absolute impedance (at 1.0 Hz) as a function of the pH in Fig. 4A shows that the resistance of the sensor changes in the pH range of 1–4 and then becomes nearly constant above pH 4. This effect can be observed in more detail in the Bode phase diagram shown in Fig. 4B for the proposed circuit. Two distinct phase angles (θ) are observed in the Bode diagram and correspond to the two semicircles observed in the complex plane plot. In the frequency range of 10^2–10^4 Hz, the phase angle decreases with decreasing pH below pH 4, indicating a change from a pseudocapacitor to a resistive component of the circuit (Fig. $2B_2$). This transformation might be due to the dominant influence of the charge transfer resistance of the sensor in this frequency range, which is revealed by the acceleration in the rate of oxygen reduction at the solution/polymer interface. However, in the lower frequency range of 10^{-1}–10^2 Hz, the phase angle exhibits an inverse relationship with pH, confirming the diffusion of the charge into the metallopolymer.

3.3. Chemiresistor sensor response to dissolved oxygen

The sensor response as a function of the dissolved oxygen concentration was determined by absolute impedance measurements and can be analyzed from the 3D Bode diagram (Fig. 5A).

The maximum changes in the impedance are observed at frequencies of less than 10 Hz, which is the region that most reflects the resistance. The absolute impedance decreases significantly to small variations of O_2 concentrations tested up to the saturation of the electrolyte solution with molecular oxygen. The decrease in the resistance is due to the increase in the electronic coupling between the cobalt sites. Fig. 5B shows the resistive response curve of the metallopolymer sensor at 0.5 Hz in the oxygen concentration range of 2.72 mg L^{-1} to 40.9 mg L^{-1} with detection limit of 0.55 mg L^{-1}. Each data point indicates the average response of three measurements of the same chemiresistor material. The sensor response is represented by Eq. (4):

$$|Z|(k\Omega) = 36.0 - 0.483 \pm 0.003[O_2](mg\ L^{-1}) \qquad (n = 13;\ R = 0.9995) \tag{4}$$

The selectivity of the chemiresistor sensor for oxygen sensing was evaluated by the following the Eq. (5):

$$\text{Relative response} = \left(\frac{\Delta S_i}{\Delta S_o}\right) x100\% \tag{5}$$

where ΔS_i is the difference in the resistance measure at interference and ΔS_o is the difference in the resistance for oxygen. Fig. 6 shows the interference study in the impedance response of the sensor. The sensor response to dissolved oxygen (41.1 mg L^{-1}) is higher than those to the other dissolved gases tested, including CO_2 (1.4 g L^{-1}), CH_4 (25 mg L^{-1}) and SO_2 (50 mg L^{-1}). Furthermore, the potential interference of substances such as hydrogen peroxide, benzoquinone, 4-nitrophenol, phenol, glucose, caffeine and ammonium, in concentration of 1 mmol L^{-1} was also evaluated (Fig. 6). The analyzed compounds

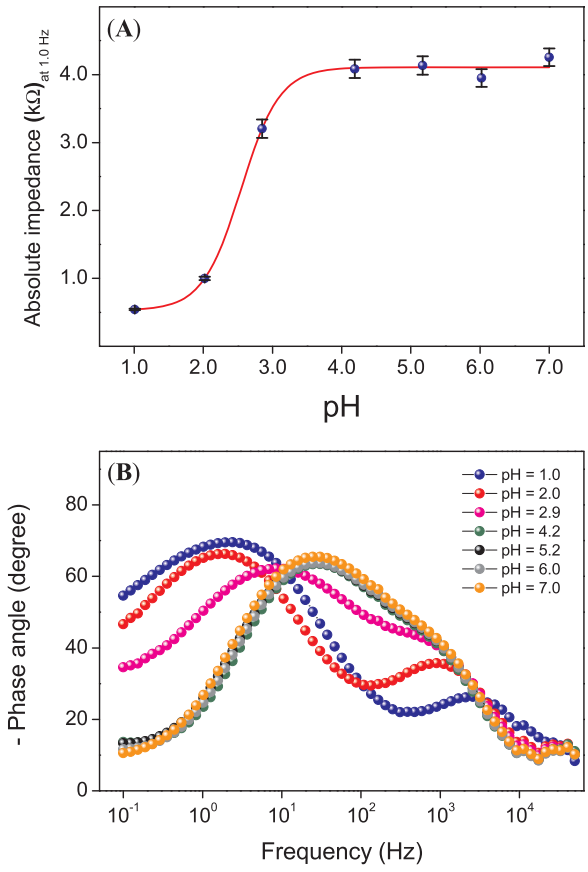

Fig. 4. (**A**) Sensor response (absolute impedance magnitude at 1.0 Hz) as a function of the pH. The error bars represent the standard deviation from three separate experiments using the same sensor. (**B**) Influence of the pH on the phase angle (Bode diagram) of the metallopolymer sensor in a 0.5 mol L^{-1} KCl solution (pH 1.0 – 7.0) saturated with O_2 (41.1 mg L^{-1}) at an applied potential of −0.2 V vs. SCE. t = 25 °C.

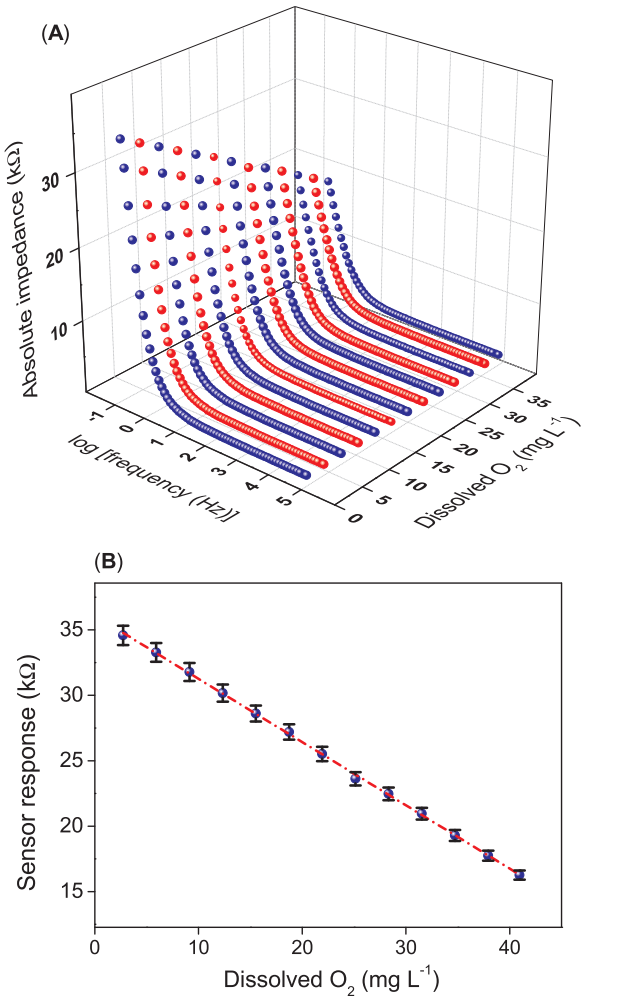

Fig. 5. (**A**) 3D Bode impedance magnitude plot recorded for the chemiresistor sensor as a function of the applied frequency at different concentrations of dissolved oxygen in the range of 2.72–40.9 mg L^{-1} in a 0. 5 mol L^{-1} KCl solution. Applied potential = -0.20 V vs. SCE. (**B**) Sensor response at 0.5 Hz. t = 25 °C. The error bars represent the standard deviation from three separate experiments using the same sensor.

were not considered to interfere when the relative response in the measured impedance was less than 5%. These results indicate that the chemiresistor sensor based on the cobalt-salen metallopolymer is a promising and sensitive platform for dissolved oxygen determination in environmental samples. As previously mentioned about the effect of pH on resistive response, the best pH working range was between pH 4 and pH 7.

The analysis of dissolved O2 for environmental water samples were realized in triplicate (n = 3). The results presented in Table 1 agreed within 95% confidence level according to the student t-test once calculated t-values were smaller than tabled t-value (2.78). The values of dissolved oxygen obtained using the chemiresistor sensor are in good agreement with those obtained using a commercial sensor demonstrating the good potential of the chemiresistor material as an oxygen sensor (Table 2).

Fig. 7A shows the response of the oxygen chemiresistor sensor in KCl solutions saturated with O_2 and N_2 at a fixed frequency of 0.5 Hz. The sensor exhibits an excellent response to dissolved oxygen, and this response is reversible and reproducibly returns to the baseline in the solution saturated with N_2. Furthermore, the sensing efficiency decreases by only 2.0% after 20 cycles. The chemiresistor sensor was also tested by exposing it to three different concentrations of dissolved O_2, and as expected, its response depends on the dissolved oxygen concentration. The steady-state response of the sensor under N_2 and O_2 for two hours was also studied. The sensor signal is constant, resulting in a response that neither rises nor falls. Fig. 7B shows the transient response of the chemiresistor during cycling between saturated O_2 and N_2 conditions. The response to oxygen is quite rapid, with an apparent

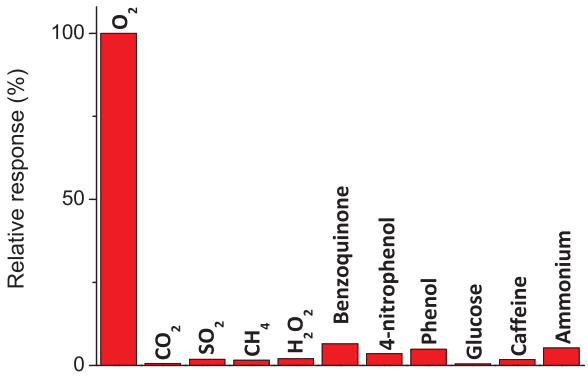

Fig. 6. Relative response of the oxygen chemiresistor sensor.

response time of ± 3 min (highlighted in the figure as the O_2 response). The recovery time (or O_2 desorption time) is ± 3 min ($time_{90\%}$). The long-term stability of the sensor was evaluated by measuring the resistance cycles in the absence and presence of O_2 at a fixed frequency of 0.5 Hz every 15 day over a period of 90 days. The resistance signal of the sensor in response to dissolved oxygen decreases by only 4.7% in 90 days.

Table 2
Statistical comparison of the results obtained with the chemiresistor and commercial O_2 sensors for the determination of dissolved oxygen. (n = 3).

Sample	Chemiresistor sensor (O_2 mg L^{-1})	Commercial sensor (O_2 mg L^{-1})	*t*-test	Error (%)
Public supply	6.38 ± 0.48	6.55 ± 0.36	0.51	+ 2.6
Carbonated water	0	0	–	–
Lake water[a]	6.70 ± 0.30	6.39 ± 0.20	1.29	− 4.8
Lake water[b]	6.77 ± 0.25	6.44 ± 0.20	1.84	− 5.1
Well water	6.67 ± 0.30	6.82 ± 0.26	0.23	+ 2.2

[a] Water collection at the edge.
[b] Water collection within 60 cm of the edge.

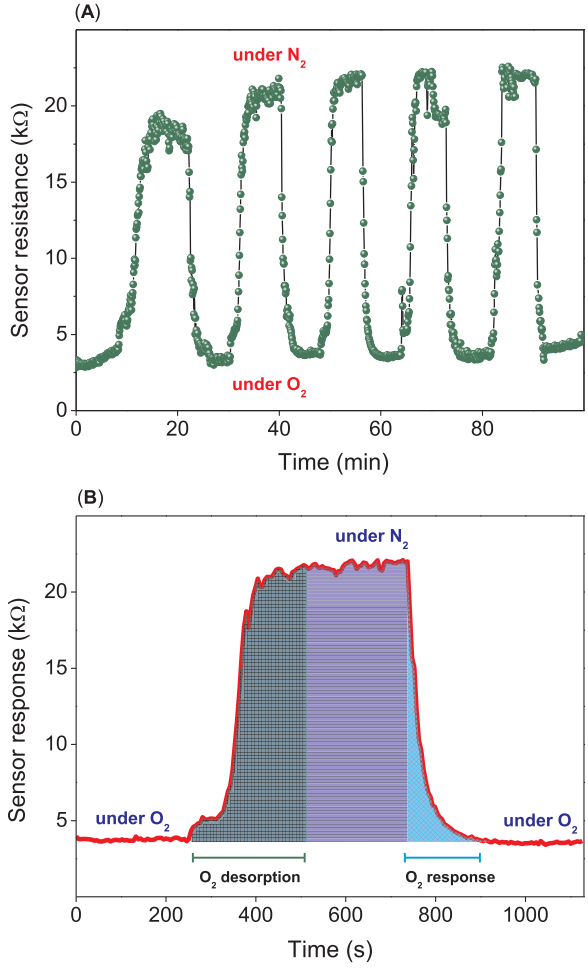

Fig. 7. (**A**) Transient responses of the oxygen sensor in a KCl solution at a fixed frequency of 0.5 Hz as a function of time. Applied potential = -0.20 V vs. SCE. (**B**) Response and recovery time under O_2 (41.1 mg L^{-1}) and N_2. *t* = 25 °C.

4. Conclusions

A chemiresistive device based on a cobalt-salen metallopolymer is demonstrated to be a simple, sensitive and selective sensor for dissolved O_2 detection in aqueous media. The mechanism relies on the reaction of molecular oxygen with the cobalt ion of the metallopolymer. The mixed valency of the cobalt results in the rapid oscillation of charge throughout the polymer chain and thus an increase in the conductivity. The resistance of the sensor decreases linearly with increasing amount of dissolved O_2 in the electrolyte solution. The sensor response is linear in the dissolved oxygen concentration range of 2.72 mg L^{-1} to 40.9 mg L^{-1}. Furthermore, the sensor exhibits a good sensitivity of 0.483 kΩ L mg^{-1} and excellent repeatability and reproducibility. Because of the complete selectivity of the metallopolymer in this sensor to oxygen, interference effects from unexpected gases in the solution are essentially zero, and thus, they will not influence the sensor performance. This sensor material can be adapted for various environmental applications. The great advantage is the design eliminates the use of semipermeable membrane as used in commercial sensor (Clark electrode).

Acknowledgment

The authors acknowledge FAPESP (2016/09017-1) for financial support. C.F. Pereira thanks CNPq-Brazil (113827/2012-1) for a fellowship. SJT ∴

Appendix A. Supporting information

Supplementary data associated with this article can be found in the online version at doi:10.1016/j.talanta.2018.07.080.

References

[1] M.A. Hanson, X.D. Ge, Y. Kostov, K.A. Brorson, A.R. Moreira, G. Rao, Comparisons of optical pH and dissolved oxygen sensors with traditional electrochemical probes during mammalian cell culture, Biotechnol. Bioeng. 97 (2007) 833–841.
[2] B.H. Junker, D.I.C. Wang, T.A. Hatton, Fluorescence sensing of fermentation parameters using fiber optics, Biotechnol. Bioeng. 32 (1988) 55–63.
[3] H. te Kulve, K. Konrad, Sectoral demand articulation: the case of emerging sensor technologies in the drinking water sector, Technol. Forecast. Soc. 119 (2017) 154–169.
[4] C.E.W. Hahn, Electrochemical analysis of clinical blood-gases, gases and vapours, Analyst 123 (1998) 57r–86r.
[5] J.D. Wadhawan, P.J. Welford, H.B. McPeak, C.E.W. Hahn, R.G. Compton, The simultaneous voltammetric determination and detection of oxygen and carbon dioxide – a study of the kinetics of the reaction between superoxide and carbon dioxide in non-aqueous media using membrane-free gold disc microelectrodes, Sens. Actuators B-Chem. 88 (2003) 40–52.
[6] S. Bellani, A. Ghadirzadeh, L. Meda, A. Savoini, A. Tacca, G. Marra, R. Meira, J. Morgado, F. Di Fonzo, M.R. Antognazza, Hybrid organic/inorganic nanostructures for highly sensitive photoelectrochemical detection of dissolved oxygen in aqueous media, Adv. Funct. Mater. 25 (2015) 4531–4538.
[7] C.S. Martin, T.R.L. Dadamos, M.F.S. Teixeira, Development of an electrochemical sensor for determination of dissolved oxygen by nickel-salen polymeric film modified electrode, Sens. Actuators B-Chem. 175 (2012) 111–117.
[8] M. Gutierrez-Capitan, A. Baldi, R. Gomez, V. Garcia, C. Jimenez-Jorquera, C. Fernandez-Sanchez, Electrochemical nanocomposite-derived sensor for the analysis of chemical oxygen demand in urban wastewaters, Anal. Chem. 87 (2015) 2152–2160.
[9] C.J. Lim, J.W. Park, Luminescent oxygen-sensing films with improved sensitivity based on light scattering by TiO2 particles, Sens. Actuators B-Chem. 253 (2017) 934–941.
[10] C.S. Chu, Y.L. Lo, Optical fiber dissolved oxygen sensor based on Pt(II) complex and core-shell silica nanoparticles incorporated with sol-gel matrix, Sens. Actuators B-Chem. 151 (2010) 83–89.
[11] T. Hyakutake, I. Okura, K. Asai, H. Nishide, Dual-mode oxygen-sensing based on oxygen-adduct formation at cobaltporphyrin-polymer and luminescence quenching of pyrene: an optical oxygen sensor for a practical atmospheric pressure, J. Mater. Chem. 18 (2008) 917–922.
[12] Y. Amao, Probes and polymers for optical sensing of oxygen, Microchim Acta 143 (2003) 1–12.
[13] T. Zhang, S. Mubeen, N.V. Myung, M.A. Deshusses, Recent progress in carbon nanotube-based gas sensors, Nanotechnology 19 (2008).
[14] R. Ramamoorthy, P.K. Dutta, S.A. Akbar, Oxygen sensors: materials, methods, designs and applications, J. Mater. Sci. 38 (2003) 4271–4282.
[15] Y. Zhou, Y.D. Jiang, T. Xie, H.L. Tai, G.Z. Xie, A novel sensing mechanism for resistive gas sensors based on layered reduced graphene oxide thin films at room temperature, Sens. Actuators B-Chem. 203 (2014) 135–142.
[16] I.A. Pasti, A.J. Lezaic, G. Ciric-Marjanovic, V.M. Mirsky, Resistive gas sensors based on the composites of nanostructured carbonized polyaniline and Nafion, J. Solid State Electr. 20 (2016) 3061–3069.
[17] C.R. Peverari, D.N. David-Parra, M.M. Barsan, M.F.S. Teixeira, Mechanistic study of the formation of multiblock pi-conjugated metallopolymer, Polyhedron 117 (2016) 415–421.
[18] C.S. Martin, W.B.S. Machini, M.F.S. Teixeira, Electropolymerization using binuclear nickel(II) Schiff base complexes bearing N4O4 donors as supramolecular building blocks, RSC Adv. 5 (2015) 39908–39915.
[19] M.F.S. Teixeira, T.R.L. Dadamos, An electrochemical sensor for dipyrone determination based on nickel-salen film modified electrode, Procedia Chem. 1 (2009)

297–300.
[20] T.R.L. Dadamos, M.F.S. Teixeira, Electrochemical sensor for sulfite determination based on a nanostructured copper-salen film modified electrode, Electrochim. Acta 54 (2009) 4552–4558.
[21] A.A.A. Emara, A.M. Ali, A.F. El-Asmy, E.M. Ragab, Investigation of the oxygen affinity of manganese(II), cobalt(II) and nickel(II) complexes with some tetradentate Schiff bases, J. Saudi Chem. Soc. 18 (2014) 762–773.
[22] T. Elder, J.J. Bozell, D. Cedeno, The effect of axial ligand on the oxidation of syringyl alcohol by Co(salen) adducts, Phys. Chem. Chem. Phys. 15 (2013) 7328–7337.
[23] D. Chen, A.E. Martell, Y.Z. Sun, New synthetic cobalt schiff-base complexes as oxygen carriers, Inorg. Chem. 28 (1989) 2647–2652.
[24] M.R. Tine, Cobalt complexes in aqueous solutions as dioxygen carriers, Coord. Chem. Rev. 256 (2012) 316–327.
[25] G.D. Liu, Z.Q. Li, S.S. Huan, G.L. Shen, R.Q. Yu, Electro-catalytic oxidation of ascorbic acid at a cobalt-salen polymer modified electrode and analytical applications, Anal. Lett. 33 (2000) 175–192.
[26] E.A. Smirnova, M.P. Karushev, A.M. Timonov, E.V. Alekseeva, O.V. Levin, V.V. Malev, New functional materials based on conductive polymer-metal complexes modified with metallic nanoelectrodes, Russ. Chem. B+ 64 (2015) 1919–1925.
[27] P.K. Sonkar, V. Ganesan, A. Prajapati, Polymeric Co(salen) scaffold for the electrochemical determination of acetaminophen in pharmaceutical sample, Ionics 22 (2016) 1741–1749.
[28] S. Djebbar-Sid, O. Benali-Baitich, J.P. Deloume, Synthesis, characterization and electrochemical behaviour of cobalt(II) and cobalt(III): O-2(-) complexes, respectively, with linear and tripodal tetradentate ligands derived from Schiff bases, J. Mol. Struct. 569 (2001) 121–128.
[29] S. Yamazaki, Y. Yamada, T. Ioroi, N. Fujiwara, Z. Siroma, K. Yasuda, Y. Miyazaki, Estimation of specific interaction between several Co porphyrins and carbon black: its influence on the electrocatalytic O-2 reduction by the porphyrins, J. Electroanal. Chem. 576 (2005) 253–259.
[30] J.T. Zhang, J.M. Hu, J.Q. Zhang, C.N. Cao, Studies of impedance models and water transport behaviors of polypropylene coated metals in NaCl solution, Prog. Org. Coat. 49 (2004) 293–301.
[31] J. Liu, L.W. Zhang, X.L. Mu, P.Q. Zhang, Studies of electrochemical corrosion of low alloy steel under epoxy coating exposed to natural seawater using the WBE and EIS techniques, Prog. Org. Coat. 111 (2017) 315–321.
[32] B.J. Holliday, T.M. Swager, Conducting metallopolymers: the roles of molecular architecture and redox matching, Chem. Commun. (2005) 23–36.
[33] W.J. Liu, W.J. Huang, C.H. Chen, M. Pink, D. Lee, Charge injection and transport in metal-containing conducting polymers: spectroelectrochemical mapping of redox activities, Chem. Mater. 24 (2012) 3650–3658.
[34] M.T. Nguyen, R.A. Jones, B.J. Holliday, Understanding the effect of metal centers on charge transport and delocalization in conducting metallopolymers, Macromolecules 50 (2017) 872–883.
[35] B. Vercelli, S. Zecchin, N. Comisso, G. Zotti, A. Berlin, E. Dalcanale, L.B. Groenendaal, Solvoconductivity of polyconjugated polymers: the roles of polymer oxidation degree and solvent electrical permittivity, Chem. Mater. 14 (2002) 4768–4774.